Vascular endothelial growth factor can signal through platelet-derived growth factor receptors

Stephen G. Ball,[1,2] C. Adrian Shuttleworth,[2] and Cay M. Kielty[1,2]

[1]UK Centre for Tissue Engineering and [2]Wellcome Trust Centre for Cell-Matrix Research, Faculty of Life Sciences, The University of Manchester, Manchester M13 9PT, England, UK

Vascular endothelial growth factor (VEGF-A) is a crucial stimulator of vascular cell migration and proliferation. Using bone marrow–derived human adult mesenchymal stem cells (MSCs) that did not express VEGF receptors, we provide evidence that VEGF-A can stimulate platelet-derived growth factor receptors (PDGFRs), thereby regulating MSC migration and proliferation. VEGF-A binds to both PDGFRα and PDGFRβ and induces tyrosine phosphorylation that, when inhibited, results in attenuation of VEGF-A–induced MSC migration and proliferation. This mechanism was also shown to mediate human dermal fibroblast (HDF) migration. VEGF-A/PDGFR signaling has the potential to regulate vascular cell recruitment and proliferation during tissue regeneration and disease.

Introduction

The vascular endothelial growth factor (VEGF) and PDGF family members are closely related. In *Drosophila melanogaster* three PDGF/VEGF-like factors (PVFs) have been identified that function through a single receptor to mediate guidance of cell migration (Duchek et al., 2001; Cho et al., 2002). A PVF identified in *Caenorhabditis elegans* was shown to bind the human VEGF receptors (VEGFRs) VEGFR1 and VEGFR2, which mediated angiogenesis (Tarsitano et al., 2006). Sequence analysis of VEGF, PDGF, and PVF members predicts that VEGF and PDGF evolved from a common ancestor (Holmes and Zachary, 2005). Both VEGF and PDGF belong to the cystine-knot superfamily of signaling molecules, which is characterized by having a cystine-knot structure formed by eight cysteine residues (Vitt et al., 2001).

The most abundant and active member of the VEGF family is VEGF-A (Holmes and Zachary, 2005; Yamazaki and Morita, 2006), which undergoes alternative splicing to produce several different isoforms. The predominant human isoforms are VEGF-A_{165} and -A_{121}, which lacks a heparin-binding domain (Neufeld et al., 1999). Three VEGFR tyrosine kinases (RTKs; VEGFR1-3) that form homodimers on ligand binding have been identified (Holmes and Zachary, 2005; Yamazaki and Morita, 2006). VEGF-A binds to VEGFR1 and VEGFR2, but not VEGFR3, but most signal transduction is mediated by VEGFR2 (Zachary and Gliki, 2001; Cross et al., 2003). All three VEGFRs are structurally related to the PDGF class III RTK subfamily, which are all characterized by seven extracellular immunoglobulin-like domains with an intracellular tyrosine kinase domain interrupted by a noncatalytic region (Petrova et al., 1999). These and other structural similarities between VEGFRs and PDGF receptors (PDGFRs) suggest a close evolutionary relationship (Kondo et al., 1998).

The PDGF family consists of four different PDGF chains (A–D), which assemble into functional homodimers or a PDGF-AB heterodimer, and two PDGFR tyrosine kinases (α and β), which form a homodimer or heterodimer on ligand binding (Betsholtz, 2004; Fredriksson et al., 2004). PDGF-AA binds only PDGFRα, whereas PDGF-BB binds both homodimer and heterodimer PDGFRs. The less abundant PDGF-CC and -DD bind to PDGFRα and PDGFRβ homodimers, respectively, with both binding to the PDGFRαβ heterodimer. PDGF-C and -D have a novel N-terminal CUB domain and are structurally more similar to the VEGF family than the PDGFs (Fredriksson et al., 2004; Reigstad et al., 2005).

VEGF-A and PDGF-BB are both critical factors in promoting the recruitment and proliferation of vascular cells (Benjamin et al., 1998; Yancopoulos et al., 2000). Adult bone marrow–derived mesenchymal stem cells (MSCs), which can differentiate to vascular cells (Galmiche et al., 1993; Kashiwakura et al., 2003; Ball et al., 2004), may be recruited during angiogenesis

Correspondence to C. Adrian Shuttleworth: adrian.shuttleworth@manchester.ac.uk; or Cay M. Kielty: cay.kielty@manchester.ac.uk

Abbreviations used in this paper: DTSSP, 3, 3′-Dithiobis[sulfosuccinimidyl propionate]; HDF, human dermal fibroblast; HUVEC, human umbilical vein endothelial cell; MSC, mesenchymal stem cell; NP, neuropilin; PDGFR, PDGF receptor; PVF, PDGF/VEGF-like factor; RTK, receptor tyrosine kinase; VEGF, vascular endothelial growth factor; VEGFR, VEGF receptor.

The online version of this article contains supplemental material.

The Journal of Cell Biology, Vol. 177, No. 3, May 7, 2007 489–500
http://www.jcb.org/cgi/doi/10.1083/jcb.200608093

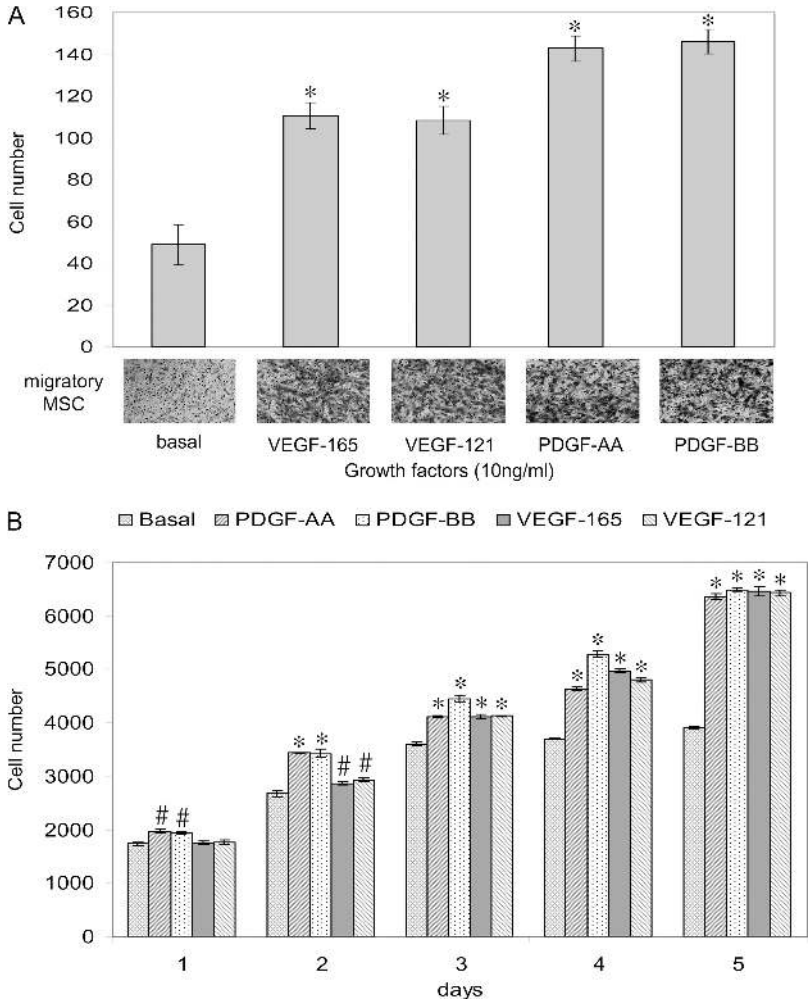

Figure 1. **Exposure to VEGF-A increased MSC migration and proliferation.** (A) MSC migration was examined in serum-free conditions after a 5-h exposure to a growth factor; 10 ng/ml VEGF-A_{165}, VEGF-A_{121}, PDGF-AA, or PDGF-BB in the lower half of a Boyden chamber. Basal represents growth factor–independent migration. Images below each bar graph are representative of migratory cells/field (using a 10× objective lens) on the membrane underside. Data shown are the mean number of migratory cells ± the SD determined from 10 random fields from each of four independent experiments. *, $P < 0.001$, compared with basal migration. (B) MSC proliferation was determined over a 5-d period after incubation with growth medium supplemented with fresh growth factor; 10 ng/ml VEGF-A_{165}, VEGF-A_{121}, PDGF-AA, or PDGF-BB every 24 h. Basal represents proliferation independent of supplemented growth factors. Data shown are the mean cell number ± the SD determined from triplicate assays from each of two independent experiments. *, $P < 0.001$; #, $P < 0.005$ compared with the respective basal cell proliferation.

and to sites of vascular injury (Shimizu et al., 2001; Abedin et al., 2004). Although PDGF isoforms induce human MSC migration (Fiedler et al., 2004), less is known of VEGF-A–mediated effects, with several studies reporting no VEGFR expression in MSCs (Furumatsu et al., 2003; Kim et al., 2005). In this investigation, we examined the role of VEGF-A in regulating MSC migration and proliferation.

We report that VEGF-A can directly signal through PDGFR, which represents a novel VEGF-A/PDGFR signaling mechanism. This study provides important new insights into how VEGF signaling regulates MSC recruitment and proliferation during tissue regeneration and disease.

Results

MSC recruitment and proliferation by vascular growth factors are critical events during blood vessel growth, repair, and disease. In this study, we examined the chemotactic and mitogenic effects of VEGF-A on MSCs.

VEGF-A–induced MSC migration and proliferation

Boyden chamber migration assays were used to analyze the chemotactic effects of 10 ng/ml VEGF-A on MSC migration. 10 ng/ml PDGF was used as a positive control. Both VEGF-A_{165} and -A_{121} isoforms significantly increased MSC migration by ~2.2-fold above basal levels (Fig. 1 A). In comparison, both PDGF-AA and -BB isoforms resulted in an ~3.3-fold increase in MSC migration (Fig. 1 A). VEGF-A–induced MSC migration was dose dependent, with both isoforms producing maximal stimulation at 10 ng/ml VEGF-A (unpublished data).

In addition to inducing MSC migration, VEGF-A also stimulated MSC proliferation. Both VEGF-A_{165} and -A_{121} isoforms (10 ng/ml) resulted in enhanced MSC proliferation by day 2 (Fig. 1 B), which significantly increased up to day 5. In comparison, PDGF-AA and -BB isoforms (10 ng/ml) significantly enhanced proliferation by day 1. Both VEGF-A and PDGF isoforms had a similar effect on MSC proliferation by day 5 (Fig. 1 B).

MSCs do not express VEGFRs

To identify which VEGFRs were expressed on MSCs, RT-PCR analysis was performed using total RNA isolated from MSCs, with human umbilical vein endothelial cells (HUVECs) and human dermal fibroblast (HDF) cells used as VEGFR-positive and -negative control cells, respectively. Using two different sets of primer pairs for each VEGFR, no VEGFR1, VEGFR2, or VEGFR3 transcripts were identified in MSC- or HDF-derived

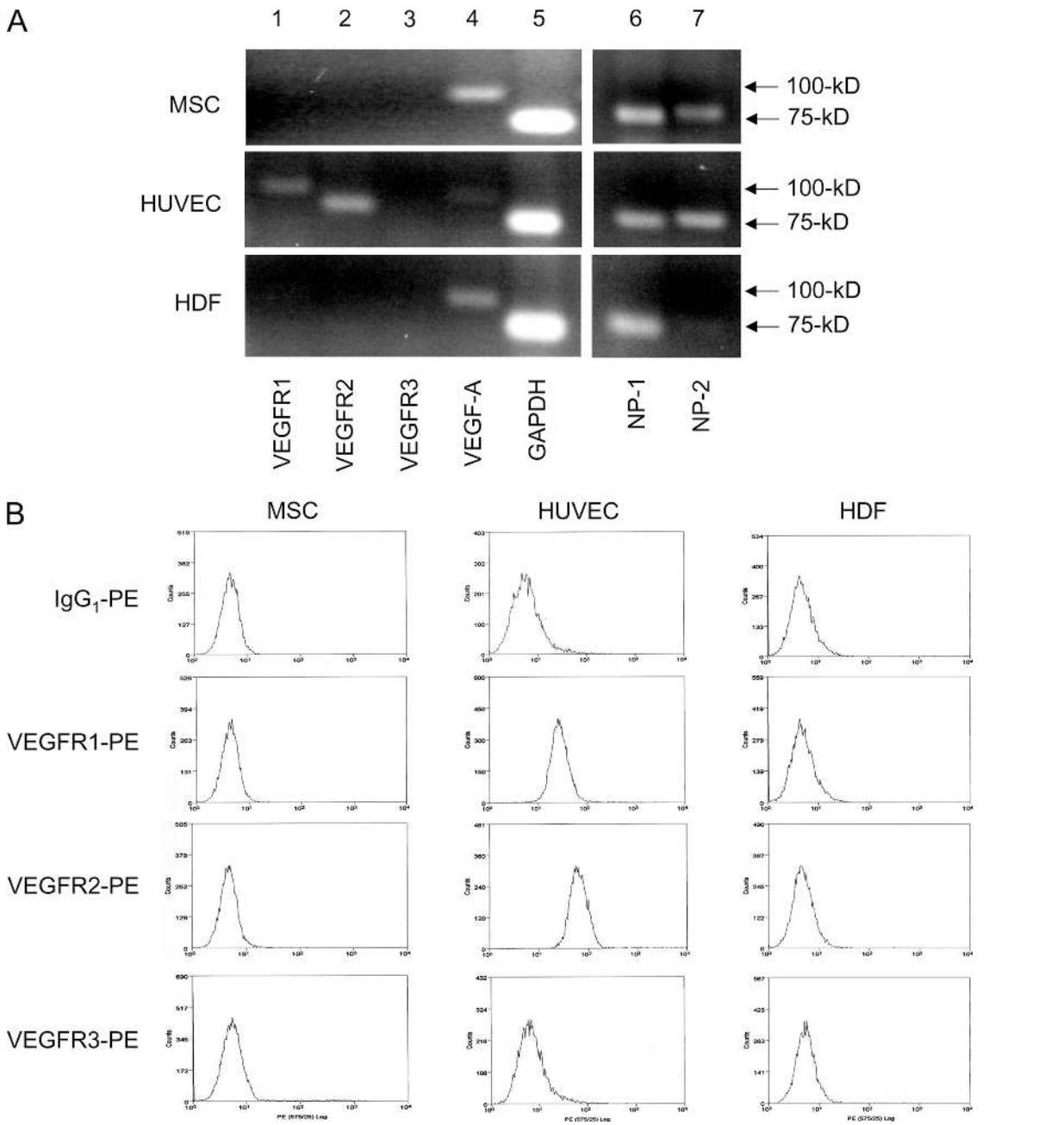

Figure 2. **MSCs expressed no VEGFRs.** The expression of VEGFR mRNA transcripts was examined by semiquantitative RT-PCR analysis and cell surface protein expression by single-color flow cytometry, using human MSCs, HUVECs as a VEGFR-positive control cell, and HDF as a VEGFR-negative control cell. (A) RNA isolated from MSCs, HUVECs, and HDFs were used to amplify VEGFR1-3, VEGF-A, NP-1, and NP-2 transcripts, with GAPDH as a control, and then resolved by agarose gel. Lane 1, VEGFR1 (99 bp); lane 2, VEGFR2 (81 bp); lane 3, VEGFR3 (87 bp); lane 4, VEGF-A (98 bp); lane 5, GAPDH (71 bp); lane 6, NP-1 (77 bp); lane 7, NP-2 (83 bp). Data are representative of six independent experiments, with two different pairs of primers for VEGFR1-3 used. (B) Flow cytometry using PE-conjugated antibodies. Analysis of VEGFR1-3 is represented by VEGFR1-, VEGFR2-, and VEGFR3-PE expression, respectively, with IgG_1-PE expression as a control. A representative example of three independent experiments is shown.

RNA (Fig. 2 A). In comparison, both VEGFR1 and VEGFR2 transcripts were readily detected in HUVECs. Although all three cell types expressed VEGF-A, MSCs had the highest abundance, but only a low level was determined in HUVECs. In addition, all three cell types also expressed neuropilin (NP)-1 and -2 coreceptor transcripts, but HDFs expressed only a trace amount of NP-2 (Fig. 2 A). Single-color flow-cytometry, using either phycoerythrin (PE)-conjugated antibodies (Fig. 2 B) or FITC-labeled antibodies (unpublished data), both demonstrated that MSCs and HDFs expressed no detectable cell surface VEGFR1, VEGFR2, or VEGFR3 protein. In comparison, HUVECs were shown to express abundant cell surface VEGFR1 and VEGFR2 (Fig. 2 B). After the end of migration assays, when MSCs had been exposed to either 10 ng/ml VEGF-A_{165} or -A_{121} for 5 h, both RT-PCR and flow cytometry analysis again demonstrated no detectable VEGFR1-3 expression

(unpublished data). Human MSCs from five different individuals were all VEGFR-negative, reflecting the lack of VEGFRs in these cells.

PDGFRα and PDGFRβ are essential for VEGF-A–induced MSC migration and proliferation

To confirm that VEGF-A–induced MSC migration was not mediated by VEGFR signaling, MSCs or HUVECs used as VEGFR-positive cells were pretreated with either specific VEGFR1 or VEGFR2 neutralization antibodies or a specific VEGFR2 tyrosine kinase inhibitor (VEGFR2-TK) before VEGF-A–induced migration. As a negative control, both cell types were also pretreated with a specific PDGFR tyrosine kinase inhibitor (PDGFR-TK). Pretreatment with either VEGFR1 or VEGFR2 neutralization antibodies or with VEGFR2-TK inhibition, all significantly decreased VEGF-A_{165}–induced HUVEC migration (Fig. 3 A). In comparison, cell surface antibody neutralization of either VEGFR1 or VEGFR2, or intracellular VEGFR2-TK inhibition, had no substantial effect on VEGF-A_{165}–induced MSC migration (Fig. 3 A). Although pretreatment with PDGFR-TK had no substantial effect on VEGF-A_{165}–induced HUVEC migration (Fig. 3 A), surprisingly, VEGF-A_{165}–induced MSC migration was significantly reduced (Fig. 3 A), indicating PDGFR involvement in VEGF-A–induced MSC migration. Similar results were obtained using isoform VEGF-A_{121} (unpublished data).

We next investigated the relationship between PDGFRs and VEGF-A–stimulated MSC migration by blocking cell surface PDGFRα or PDGFRβ, using selective neutralization antibodies. MSCs, or HUVECs used as a VEGFR-positive cell, were pretreated with either a PDGFRα- or PDGFRβ-specific neutralization antibody before VEGF-A–induced migration. Blocking either cell surface PDGFRα or PDGFRβ significantly inhibited VEGF-A_{165}– or VEGF-A_{121}–induced MSC migration (Fig. 3 A and not depicted), with PDGFRα neutralization resulting in greater inhibition of VEGF-A stimulation. In comparison, neither PDGFRα nor PDGFRβ neutralization

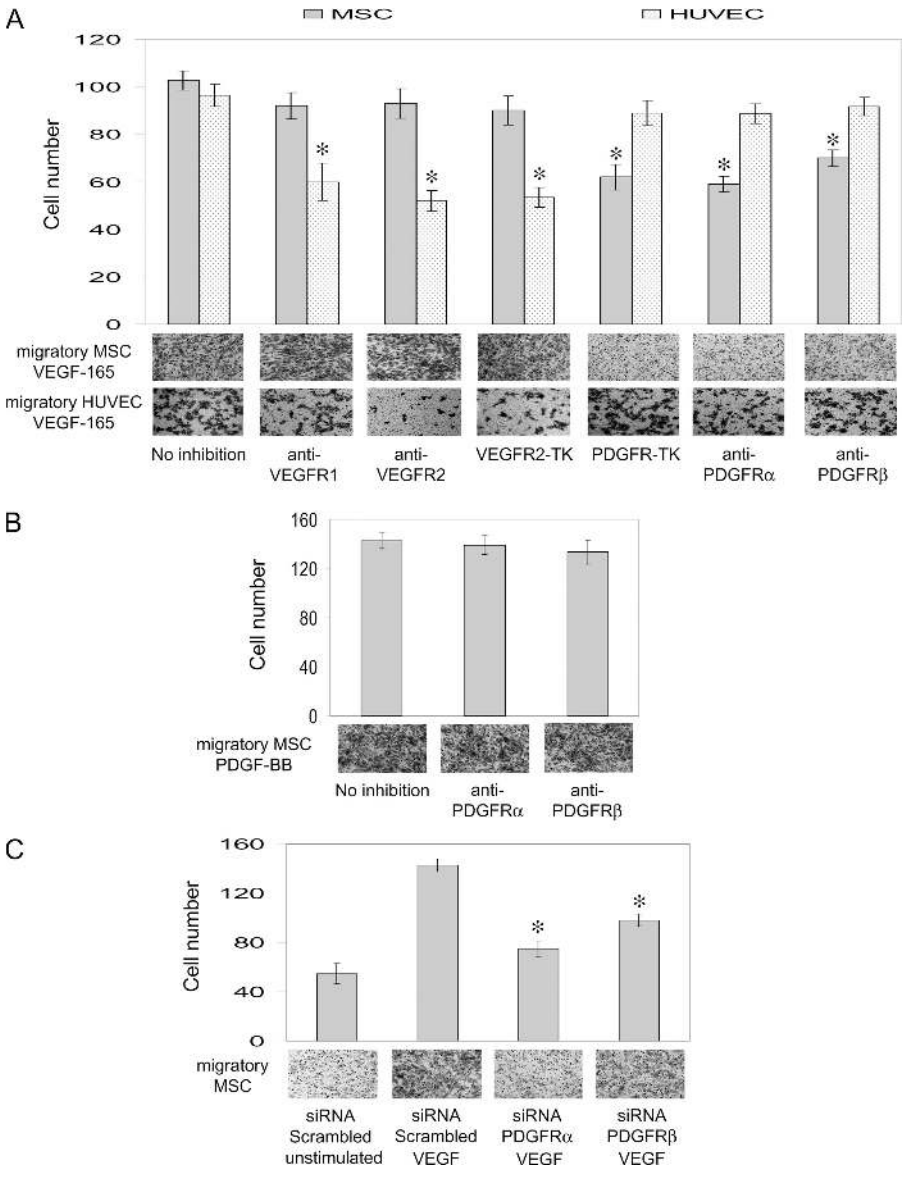

Figure 3. **Inhibiting PDGFRα or PDGFRβ attenuated VEGF-A–induced MSC migration.** (A) MSCs, or HUVECs used as a VEGFR-positive cell, were pretreated with either 10 μg/ml anti-VEGFR1 or -VEGFR2 neutralization antibodies, 100 nM VEGFR2 tyrosine kinase inhibitor (VEGFR2-TK), 2 μM PDGFR tyrosine kinase inhibitor (PDGFR-TK), and 10 μg/ml anti-PDGFRα or -PDGFRβ neutralization antibodies; then, either 10 ng/ml VEGF-A_{165} or 10 ng/ml VEGF-A_{121} (not depicted) were added to the lower half of a Boyden chamber for 5 h. No inhibition represents control VEGF-A–induced migration. (B) As a control, MSCs were pretreated with either 10 μg/ml anti-PDGFRα or -PDGFRβ neutralization antibodies, and then 10 ng/ml PDGF-BB was added to the lower half of a Boyden chamber for 5 h. No inhibition represents control PDGF-BB–induced migration. (C) MSCs were transfected with either 3 μg siRNA PDGFRα, siRNA PDGFRβ, or scrambled siRNA used as a control. Transfected MSCs in serum-free conditions were either unstimulated as a control, or exposed to 10 ng/ml VEGF-A_{165} in the lower half of a Boyden chamber for 5 h. Images below each bar graph are representative of migratory cells/field (using a 10× objective lens) on the membrane underside. Data shown are the mean number of migratory cells ± the SD, which were determined from 10 random fields from each of four (A) or two (B and C) independent experiments. *, $P < 0.001$, compared with the respective uninhibited VEGF-A_{165}–stimulated cells.

had any substantial impact on VEGF-A_{165}–induced HUVEC migration (Fig. 3 A) or PDGF-BB–induced MSC migration (Fig. 3 B). Thus, functional cell surface PDGFRα and PDGFRβ are both crucial determinants in mediating VEGF-A–induced MSC migration.

To further demonstrate that both PDGFRα and PDGFRβ are crucial receptors in directing VEGF-A–induced MSC migration, we used specific validated siRNA PDGFRα and PDGFRβ nucleotides to knockdown the respective transcripts. VEGF-A_{165} stimulation of MSCs transfected with scrambled siRNA as a control resulted in an ∼2.5-fold increase in migration above unstimulated scrambled siRNA control levels (Fig. 3 C). However, VEGF-A_{165} stimulation of MSCs transfected with either siRNA PDGFRα or PDGFRβ both resulted in a significant inhibition of migration (Fig. 3 C). Thus, PDGFRα or PDGFRβ inhibition by siRNA knockdown or cell surface neutralization (Fig. 3 A) both effectively inhibited VEGF-A_{165}–induced migration.

Having demonstrated that 5-d exposure to VEGF-A_{165} significantly enhanced MSC proliferation (Fig. 1 B), we stimulated MSCs with VEGF-A_{165} in the presence of either PDGFRα or PDGFRβ neutralization antibodies, and then examined the effects on proliferation at day 5. Blocking cell surface PDGFRα or PDGFRβ significantly inhibited VEGF-A_{165}–induced MSC proliferation (Fig. S1, available at http://www.jcb.org/cgi/content/full/jcb.200608093/DC1). In comparison, neither VEGFR1 nor VEGFR2 neutralization antibodies had any substantial impact on VEGF-A_{165}–induced MSC proliferation (Fig. S1). Thus, functional cell surface PDGFRα and PDGFRβ are both essential in mediating VEGF-A–induced MSC migration and proliferation.

VEGF-A–induced HDF migration was also mediated by PDGFRα and PDGFRβ

Having confirmed that HDFs did not express VEGFR transcripts or cell surface receptors (Fig. 2), we wished to establish whether

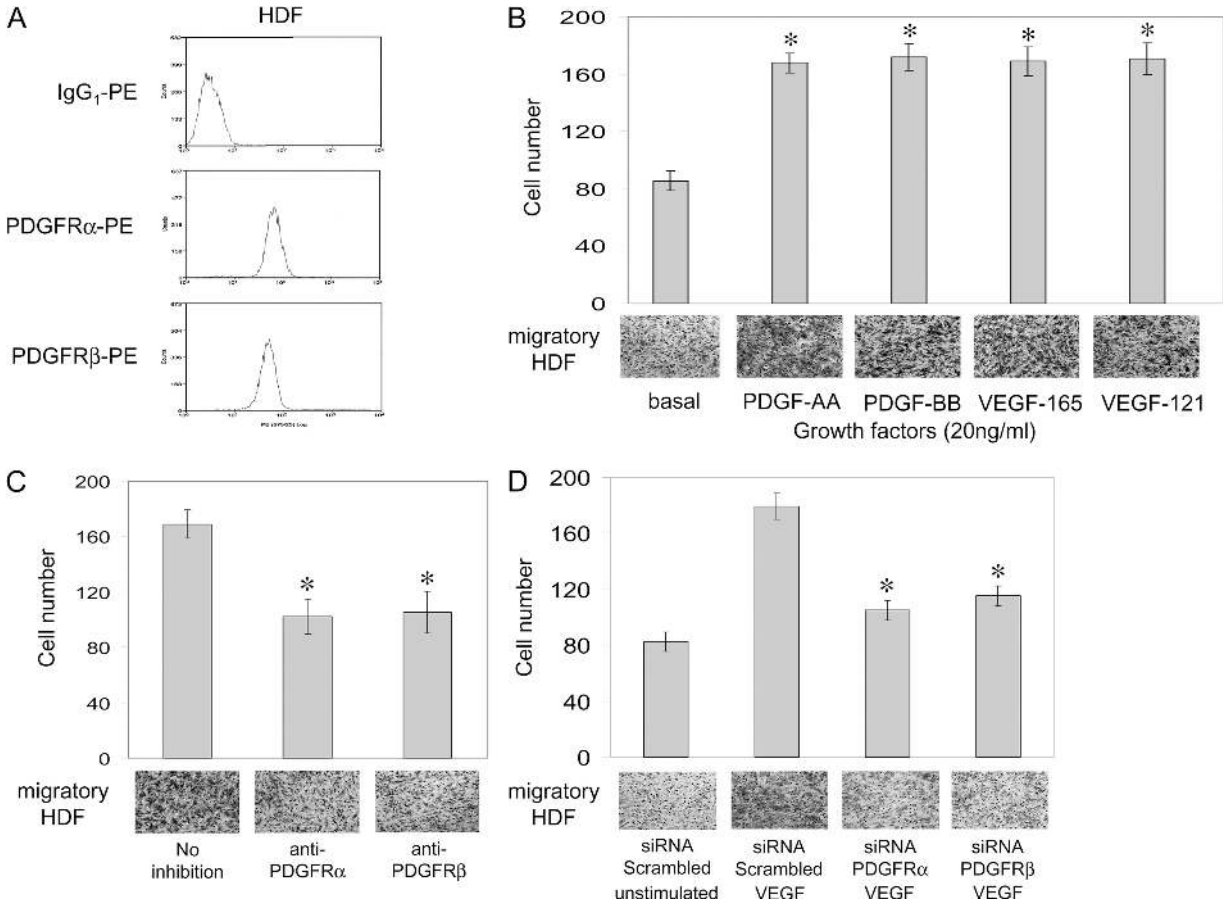

Figure 4. **VEGF-A–induced HDF migration was PDGFRα and PDGFRβ dependent.** (A) The expression of cell surface PDGFRs on HDFs were determined by single-color flow cytometry. Analysis of PDGFRα and PDGFRβ was performed using anti–human PE-conjugated antibodies, using an IgG_1-PE antibody as a control. (B) The effects of VEGF-A on HDF migration and the involvement of PDGFRs were examined using Boyden chamber migration assays. HDF migration was evaluated in serum-free conditions after 5-h exposure to growth factor; 20 ng/ml VEGF-A_{165}, VEGF-A_{121}, PDGF-AA, or PDGF-BB in the lower half of a Boyden chamber. Basal represents growth factor–independent migration. (C) HDFs were pretreated with either 10 μg/ml anti-PDGFRα or -PDGFRβ neutralization antibodies, before adding 20 ng/ml VEGF-A_{165} to the lower half of a Boyden chamber for 5 h. No inhibition represents control VEGF-A_{165}–induced migration. (D) HDFs were transfected with either 3 μg siRNA PDGFRα, siRNA PDGFRβ, or scrambled siRNA used as a control. Transfected HDFs in serum-free conditions were either unstimulated as a control, or exposed to 20 ng/ml VEGF-A_{165} in the lower half of a Boyden chamber for 5 h. Images below each bar graph are representative of migratory cells/field (using a 10× objective lens) on the underside of the membrane. Data shown are the mean number of migratory cells ± the SD determined from 10 random fields from each of three independent experiments. *, $P < 0.001$, compared with the respective uninhibited VEGF-A_{165} or PDGF-stimulated cells.

VEGF-A could also induce HDF migration by a PDGFR-dependent mechanism. Flow cytometry demonstrated that HDFs expressed abundant cell surface PDGFRα and PDGFRβ (Fig. 4 A). Boyden chamber migration analysis demonstrated that both VEGF-A_{165} and -A_{121} isoforms significantly induced a similar level of HDF migration as either PDGF-AA or -BB; the level of migration was ∼2.0-fold above basal levels (Fig. 4 B). Selectively inhibiting either PDGFRα or PDGFRβ using specific cell surface neutralization antibodies before growth factor exposure significantly inhibited VEGF-A_{165}– and -A_{121}–induced HDF migration (Fig. 4 C and not depicted). The involvement of both PDGFRα and PDGFRβ in mediating VEGF-A_{165}–induced HDF migration was further demonstrated by siRNA PDGFR knockdown. VEGF-A_{165} stimulation of HDFs transfected with scrambled siRNA as a control produced a 2.2-fold increase in migration above unstimulated control level, whereas siRNA knockdown of either PDGFRα or PDGFRβ resulted in a significant inhibition of VEGF-A_{165}–induced HDF migration (Fig. 4 D). Thus, both VEGF-A_{165}–induced MSC and HDF migration were dependent on a PDGFR-mediated mechanism.

VEGF-A_{165}–induced PDGFRα and PDGFRβ tyrosine phosphorylation

Ligand binding to a PDGFR induces receptor dimerization, which is a prerequisite for autophosphorylation of specific tyrosine residues and initiation of signal transduction (Heldin and Westermark, 1999). Having clearly demonstrated the involvement of both PDGFRs in VEGF-A–induced MSC and HDF migration, we next examined whether VEGF-A_{165} resulted in PDGFR tyrosine autophosphorylation by using a human phospho-RTK array containing 42 different specific RTK antibodies. This approach not only allowed the simultaneous relative quantitation of both PDGFR tyrosine phosphorylation levels, but also detected tyrosine phosphorylation of 40 other RTKs, including all three VEGFRs, in the same isolated cell lysate. Furthermore, this approach was an effective means to validate the efficiency of siRNA knockdown to inhibit PDGFR signaling.

RTK array analysis demonstrated that unstimulated MSC lysate resulted in all 42 different RTKs having a very low basal level of tyrosine phosphorylation (Fig. 5 A).

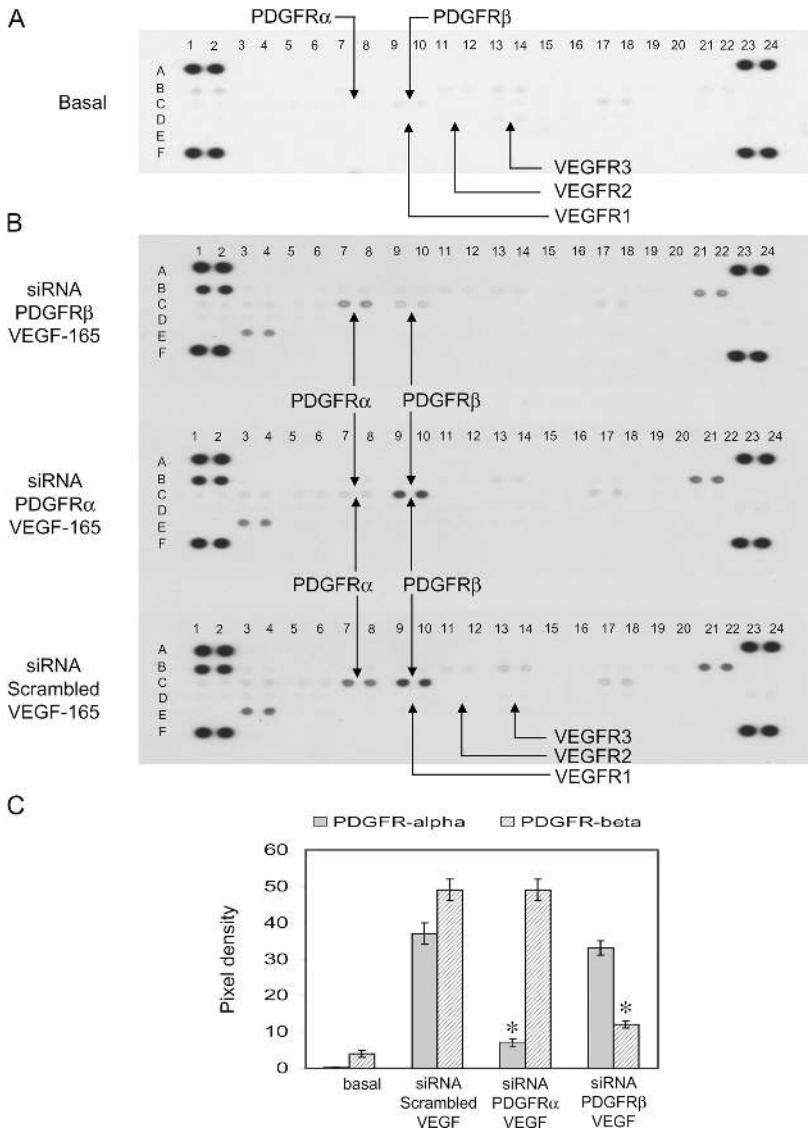

Figure 5. **VEGF-A stimulated both PDGFRα and PDGFRβ tyrosine phosphorylation.** Human phospho-RTK arrays were used to examine VEGF-A–induced RTK phosphorylation levels in MSC lysate samples. Arrays contain phosphotyrosine-positive control spots in each corner, having coordinates (A1, A2), (A23, A24), (F1, F2), (F23, F24), which were assigned a pixel density value of 100, which was used to normalize positive RTK spot pixel density values. Relevant RTK duplicate spot coordinates: PDGFRα = (C7, C8), PDGFRβ = (C9, C10), VEGFR1 = (D9, D10), VEGFR2 = (D11, D12), VEGFR3 = (D13, D14), EGFR = (B1, B2), FGFR3 = (B13, B14), Axl = (B21, B22), EphA7 = (E3, E4). (A) RTK array analysis of control MSC lysate, not stimulated with exogenous growth factor (basal). (B) RTK array analysis of lysates from MSCs transfected with 3 μg scrambled siRNA as a control, siRNA PDGFRα or siRNA PDGFRβ, stimulated using 20 ng/ml VEGF-A_{165} in serum-free conditions for 10 min at 37°C. Each array was identically exposed to detection reagents and film. (C) Bar graph representing data from arrays (A and B). Mean pixel density ± the SD of duplicate spots, normalized against duplicate phosphotyrosine-positive control spots = 100. A representative example of two independent experiments is shown for each array analysis. *, $P < 0.001$ compared with the respective VEGF-A_{165}–stimulated scrambled siRNA control.

When MSCs transfected with scrambled RNA (control) were stimulated with VEGF-A_{165} for 10 min, RTK array analysis demonstrated that the cell lysate contained distinct PDGFRα and PDGFRβ tyrosine phosphorylation (densitometry values = 37 ± 3 and 49 ± 3, respectively; Fig. 5 B). Thus, VEGF-A_{165} specifically activates both PDGFRα and PDGFRβ RTK signaling activities. Importantly, no VEGFR1-3 receptor tyrosine phosphorylation was detected, further verifying that VEGF-A stimulation of MSCs is not mediated by VEGFRs (Fig. 5 B).

After siRNA PDGFRα or PDGFRβ knockdown, followed by VEGF-A_{165} stimulation, array analysis demonstrated that the cell lysate contained a significant decrease in the tyrosine phosphorylation state of PDGFRα (densitometry value = 7 ± 1) and PDGFRβ (densitometry value = 12 ± 1), respectively (Fig. 5, B and C). Thus, VEGF-A_{165} stimulated dimerization and activation of both PDGFRα and PDGFRβ receptors. Interestingly, VEGF-A_{165} stimulation also induced tyrosine phosphorylation of other RTKs, notably EGFR, EphA7, and Axl (Fig. 5 B).

Stimulation with PDGF-BB, which is the normal ligand for both PDGFRα and PDGFRβ, was also examined. This allowed a comparison with the level of VEGF-A_{165}–stimulated PDGFRα and PDGFRβ tyrosine phosphorylation, and also further validated the siRNA PDGFR knockdown efficiency and specificity. After siRNA PDGFRα or PDGFRβ knockdown, followed by PDGF-BB stimulation, the results demonstrated that the respective siRNA PDGFRα and PDGFRβ knockdowns were both effective and specific (Fig. 6 A), validating their corresponding effects in inhibiting VEGF-A_{165}–induced MSC and HDF migration (Fig. 3 C and Fig. 4 D). Using MSCs transfected with scrambled siRNA, followed by PDGF-BB stimulation, array analysis of the cell lysate demonstrated both PDGFRα and PDGFRβ tyrosine phosphorylation (densitometry values = 81 ± 6 and 294 ± 12, respectively; Fig. 6 A). Thus, whereas 20 ng/ml VEGF-A_{165} induced similar levels of PDGFRα and PDGFRβ tyrosine phosphorylation (Fig. 5 B), in comparison, 20 ng/ml PDGF-BB induced 2.2- ± 0.1-fold and 6.0- ± 0.2-fold higher levels of PDGFRα and PDGFRβ tyrosine phosphorylation, respectively (Fig. 6 B).

Immunoprecipitation analysis also demonstrated that VEGF-A_{165} increased PDGFRα and PDGFRβ tyrosine phosphorylation levels, compared with the unstimulated basal state (Fig. 6 C). Although 20 ng/ml PDGF-BB induced a similar level

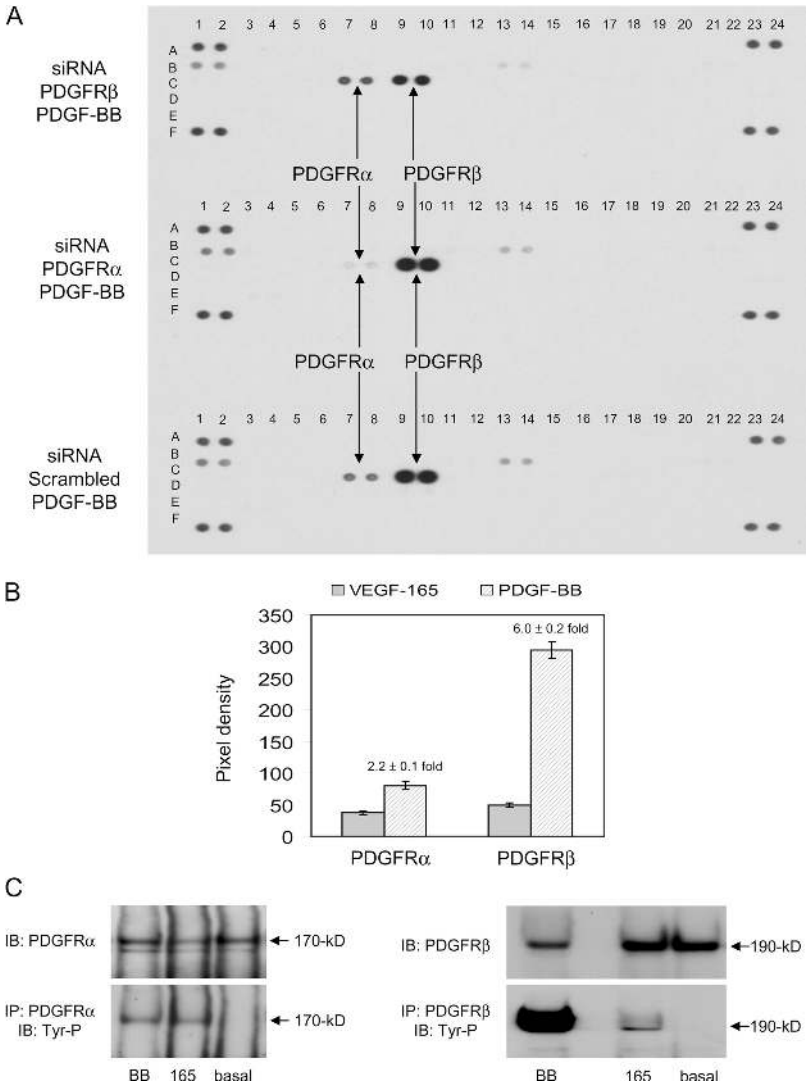

Figure 6. **VEGF-A–induced PDGFR tyrosine phosphorylation was comparable to PDGF-BB–induced PDGFRα level.** (A) RTK array analysis of lysates from MSCs transfected with 3 μg scrambled siRNA as a control, siRNA PDGFRα or siRNA PDGFRβ, stimulated using 20 ng/ml PDGF-BB in serum-free conditions for 10 min at 37°C. Each array was identically exposed to detection reagents and film. A representative example of two independent experiments is shown. (B) Bar graph comparing VEGF-A_{165}– and PDGF-BB–induced PDGFR tyrosine phosphorylation levels. Data represent VEGF-A_{165} and PDGF-BB–stimulated controls from RTK array analysis shown in Fig. 5 B and Fig. 6 A, respectively. Mean pixel density ± the SD of duplicate spots, normalized against duplicate phosphotyrosine-positive control spots = 100. (C) Immunoprecipitation (IP) analysis of PDGFR tyrosine phosphorylation levels. MSCs in serum-free conditions were unstimulated with growth factor (basal), or stimulated with either 20 ng/ml VEGF-A_{165} or PDGF-BB as a control, for 10 min at 37°C. PDGFRs were isolated from MSC lysates by IP analysis using anti-PDGFRα or anti-PDGFRβ, and then tyrosine phosphorylation detected by immunoblot (IB) analysis using anti-phosphotyrosine (Tyr-P). Membranes were reprobed with corresponding anti-PDGFRα or anti-PDGFRβ as loading controls. A representative of two independent experiments is shown.

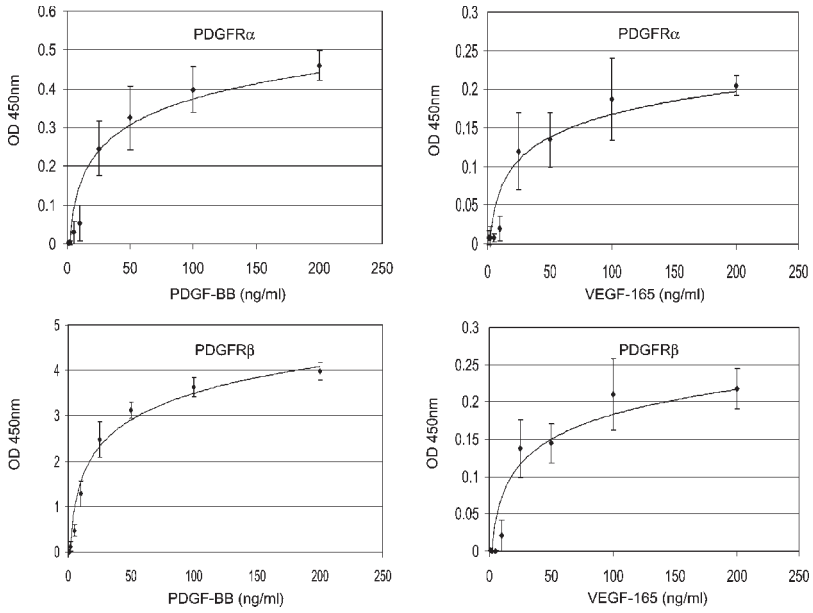

Figure 7. **VEGF-A induced a dose-dependent increase in PDGFR tyrosine phosphorylation.** The effects of varying VEGF-A_{165} concentration on induced PDGFR tyrosine phosphorylation levels was determined by specific ELISAs. MSCs in serum-free conditions were exposed to 0.5, 1, 2, 5, 10, 25, 50, 100, or 200 ng/ml VEGF-A_{165} for 10 min at 37°C. As a control, cells were also exposed to identical concentrations of PDGF-BB. MSC lysates were assayed for either PDGFRα or PDGFRβ tyrosine phosphorylation using a corresponding ELISA. Increased tyrosine phosphorylation is represented by an increase in optical density (OD_{450nm}). Data shown are mean OD_{450nm} ± the SD determined from two independent experiments performed in triplicate.

of PDGFRβ tyrosine phosphorylation to that demonstrated using RTK array analysis (Fig. 6, A and B), 20 ng/ml PDGF-BB or VEGF-A_{165} induced comparable levels of PDGFRα tyrosine phosphorylation (Fig. 6 C). Thus, both RTK array and immunoprecipitation analyses show that VEGF-A_{165}–induced PDGFR tyrosine phosphorylation levels are similar in magnitude to PDGF-BB–stimulated PDGFRα.

VEGF-A induced a dose-dependent increase in PDGFR tyrosine phosphorylation

To further examine the effects of VEGF-A on PDGFR tyrosine phosphorylation levels, MSCs were exposed to increasing concentrations of VEGF-A_{165} or PDGF-BB as a positive control. Both VEGF-A_{165} and PDGF-BB produced a dose-dependent increase in PDGFRα and PDGFRβ tyrosine phosphorylation levels (Fig. 7). In the case of VEGF-A_{165}, the minimum concentration required to induce a detectable increase in PDGFRα or PDGFRβ tyrosine phosphorylation was 10 ng/ml (Fig. S2, available at http://www.jcb.org/cgi/content/full/jcb.200608093/DC1). In comparison, PDGFRα and PDGFRβ were initially stimulated using 5 and 2 ng/ml PDGF-BB, respectively (Fig. S2). Thus, the data further highlight the comparable tyrosine phosphorylation levels induced by PDGF-BB stimulating PDGFRα and by VEGF-A_{165} stimulating either PDGFRα or PDGFRβ.

VEGF-A_{165} did not induce PDGF-BB expression or release

We have previously demonstrated that MSCs do not express PDGF-B mRNA, and VEGF-A_{165} exposure did not stimulate either PDGF-A, -B, -C, or -D transcript expression (Ball et al., 2007). Furthermore, we demonstrated by ELISA that VEGF-A exposure did not increase the level of soluble PDGF-BB (which binds to both PDGFRs) in the medium (Fig. S3, available at http://www.jcb.org/cgi/content/full/jcb.200608093/DC1).

VEGF-A_{165} bound to both PDGFRα and PDGFRβ

Having established by several methods that VEGF-A_{165}–stimulated tyrosine phosphorylation of both PDGFRs, we went on to confirm VEGF-A_{165} binding to cell surface PDGFRα and PDGFRβ using a cross-linking approach. After VEGF-A_{165} stimulation, PDGFR immunoprecipitation, and immunoblot analysis, a distinct association between VEGF-A and PDGFRα or PDGFRβ was demonstrated (Fig. 8 A). Cell surface inhibition of either PDGFRα or PDGFRβ using specific neutralization

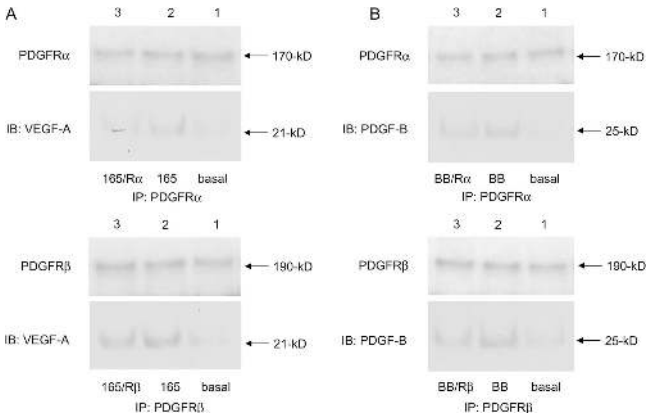

Figure 8. **VEGF-A associated with both PDGFRα and PDGFRβ.** Binding of VEGF-A to either PDGFRα or PDGFRβ was examined using a cross-linking approach. MSCs were unstimulated (basal) or stimulated with either 10 ng/ml VEGF-A_{165} (165) or PDGF-BB (BB) as a positive control, or 10 ng/ml TGF-β_1 as a negative control (not depicted), for 10 min at 37°C. To inhibit growth factor binding to the respective PDGFR, MSCs were also pretreated with either 10 μg/ml anti-PDGFRα (Rα) or -PDGFRβ (Rβ) cell surface neutralization antibodies for 30 min at 37°C, before growth factor stimulation. Growth factor binding to PDGFR was captured by adding 1 mM of a cell membrane–impermeable cross-linking agent (DTSSP), followed by immunoprecipitation (IP) analysis using anti-PDGFRα or anti-PDGFRβ, then growth factor association detected by immunoblot (IB) analysis using corresponding (A) anti–VEGF-A or (B) –PDGF-B. Membranes were reprobed with anti-PDGFRα or -PDGFRβ as loading controls. A representative of three independent experiments is shown for each analysis.

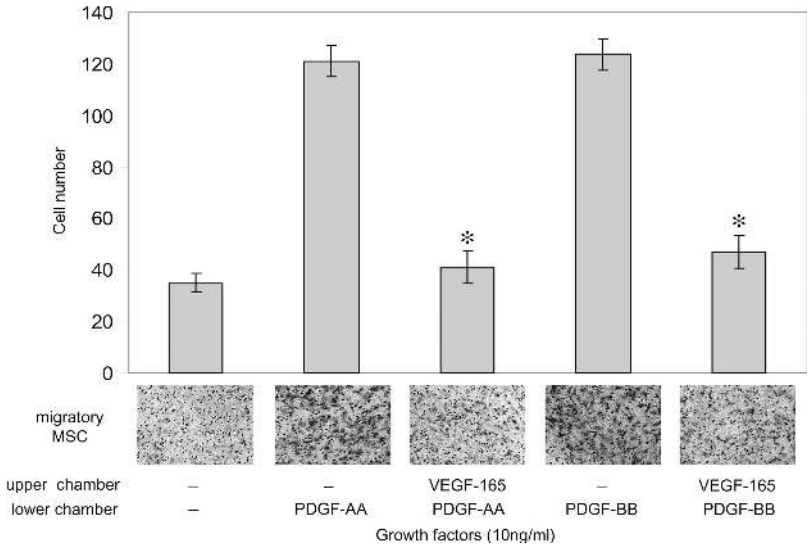

Figure 9. **PDGF-induced MSC migration was inhibited by VEGF-A.** The effects of VEGF-A on PDGF-induced MSC migration was examined using Boyden chamber migration assays. MSCs were preincubated with 10 ng/ml VEGF-A_{165} for 10 min, before adding the cell suspension onto the upper chamber membrane surface and exposure to 10 ng/ml PDGF-AA or -BB in the lower half of a Boyden chamber for 5 h. MSCs not exposed to either growth factor represents a growth factor–independent migration control. Images below each bar graph are representative of migratory cells/field (using a 10× objective lens) on the membrane underside. Data shown are the mean number migratory cells ± the SD determined from 10 random fields from each of two independent experiments. *, $P < 0.001$ compared with the respective migration induced by PDGF alone.

antibodies before growth factor stimulation resulted in decreased VEGF-A association with the corresponding PDGFR (Fig. 8 A), demonstrating the specificity of the interaction. Reprobing the membranes using anti–PDGF-B produced no immunoreactivity (unpublished data). Using the same approach, PDGF-BB (which binds both PDGFRs) stimulation as a positive control demonstrated that both PDGFRs associated with PDGF-BB (Fig. 8 B). In addition, TGF-β_1 stimulation used as a negative control, immunoprecipitated with anti-PDGFRβ, and immunoblotted using anti–TGF-β_1 showed no detectable TGF-β_1 association with PDGFRβ (unpublished data), further demonstrating the specificity of the analysis.

VEGF-A_{165} inhibited PDGF-induced MSC migration

To examine the potential competition between VEGF-A and PDGF ligands to bind PDGFRs, we performed Boyden chamber migration assays in the presence of varying concentration ratios of VEGF-A_{165} and PDGF-AA, which only binds to PDGFRα, or PDGF-BB, which binds to both PDGFRα and PDGFRβ. 10 ng/ml of either PDGF-AA or -BB in the lower half of a Boyden chamber significantly increased MSC migration above growth factor–independent basal levels (Fig. 9), as previously shown (Fig. 1 A). However, when the cell suspension in the upper half of a Boyden chamber was preincubated with 10 ng/ml VEGF-A_{165}, MSC migration toward either 10 ng/ml PDGF-AA or -BB in the lower chamber was significantly inhibited (>90% and >85% inhibition, respectively; Fig. 9). Higher ratios of VEGF-A_{165}/PDGF also resulted in similar inhibition of PDGF-induced migration (unpublished data). Thus, VEGF-A_{165} attenuation of both PDGF-AA– and -BB–induced migration demonstrated VEGF-A_{165} inhibition of both PDGFRα and PDGFRβ, providing further evidence for VEGF-A binding to both PDGFRs.

Discussion

In this study, we demonstrate that VEGF-A regulates MSC migration and proliferation, despite the fact that RT-PCR or flow cytometry analysis provided no evidence for VEGFR1-3 expression. Furthermore, using a human phospho-RTK array, which is more sensitive than immunoprecipitation, VEGF-A_{165} resulted in no detectable VEGFR1-3 tyrosine phosphorylation. However, VEGF-A–induced PDGFRα and PDGFRβ tyrosine phosphorylation was clearly confirmed, highlighting that VEGF-A exerts its effect on MSCs by the stimulation of PDGFRs.

Using complementary approaches, we provide evidence of a novel VEGF-A/PDGFR signaling mechanism, showing that VEGF-A can signal using both PDGFRs. Heparin-binding domains are important modulators of VEGF subtype binding and biological activity, VEGF-A_{165} binds heparin, but VEGF-A_{121} does not (Wijelath et al., 2006; Yamazaki and Morita, 2006). Because we demonstrated that both VEGF-A isoforms stimulated MSC and HDF migration, heparin binding is unlikely to be an important determinant. Pretreatment of MSCs with a PDGF RTK inhibitor significantly reduced VEGF-A–stimulated MSC migration. Neutralizing either cell surface PDGFRα or PDGFRβ using a specific blocking antibody also resulted in significant inhibition of VEGF-A–induced migration. Furthermore, blocking either PDGFRα or PDGFRβ expression using siRNA oligonucleotides significantly attenuated VEGF-A–induced migration, with RTK array analysis confirming decreased tyrosine phosphorylation of the respective PDGFRs. Thus, both PDGFRs are essential for VEGF-A–induced migration, suggesting that both PDGFR homodimers (-αα and -ββ) and/or a heterodimer (-αβ) mediate VEGF-A/PDGFR signaling.

PDGFRα neutralization by antibody blocking or siRNA knockdown resulted in a greater decrease in VEGF-A–induced migration than corresponding PDGFRβ inhibition, which may reflect VEGF-A binding affinity to PDGFRα. We have previously shown that the MSCs used in this study express abundant PDGFRα, have a high ratio of PDGFRα to PDGFRβ, and, importantly, virtually every cell coexpressed both receptors (Ball et al., 2007). The two PDGFRs have different PDGF binding affinities; PDGFRβ has a higher affinity for PDGF-B or -D, whereas PDGFRα has a higher affinity for PDGF-A or -C (Betsholtz et al., 2004). PDGF-C and -D are structurally more

similar to VEGF-A than to PDGF-A or -B (Reigstad et al., 2005), and both bind to a PDGFRαβ heterodimer (Fredriksson et al., 2004). MSCs exposed to PDGF-BB resulted in PDGFRα and PDGFRβ tyrosine phosphorylation levels being 2.2- and 6.0-fold higher, respectively, than corresponding VEGF-A–stimulated receptors. In comparison, VEGF-A induced similar levels of PDGFRα and PDGFRβ tyrosine phosphorylation, which may reflect a preference for PDGFRαβ stimulation. Thus, the data suggest that heterodimeric PDGFRαβ, at least in part, mediates VEGF-A/PDGFR signaling. The biological functions of PDGF-activated heterodimeric PDGFRαβ are not defined (Fredriksson et al., 2004).

Interestingly, phospho-RTK array analysis revealed that in addition to VEGF-A_{165}–induced PDGFRα and PDGFRβ tyrosine phosphorylation, VEGF-A_{165} stimulated EGFR, EphA7, and Axl tyrosine phosphorylation. PDGF-BB also stimulated EGFR phosphorylation, as well as FGFR3, but not EphA7 or Axl receptors, indicating that EphA7- and Axl-induced tyrosine phosphorylation were VEGF-A specific. Because siRNA knockdown of either PDGFRα or PDGFRβ had little impact on EphA7 or Axl tyrosine phosphorylation levels, the mechanism of VEGF-A–induced, ligand-independent dimerization and activation of EphA7 and Axl receptors remains to be determined.

We demonstrated that either VEGF-A_{165} or -A_{121} isoforms were able to induce MSC and HDF migration, and that both cell types expressed NP-1 and -2 transmembrane glycoproteins. Although VEGF-A_{165} binds to NP-1 and -2, VEGF-A_{121} binds to neither (Gluzman-Poltorak et al., 2000). NPs are not known to signal independently after VEGF binding, but are proposed to act as coreceptors and facilitate binding of certain VEGF subtypes to VEGFRs (Neufeld et al., 2002). Thus, although we cannot discount a role for NPs, in the absence of VEGFRs, to facilitate VEGF-A_{165} binding to PDGFRs, NPs are unlikely to be involved in mediating VEGF-A_{121}–induced chemotactic or mitogenic effects.

Along with finding that VEGF-A_{165} was able to induce MSC migration, we also demonstrated that a low concentration of VEGF-A_{165} at the cell surface can inhibit both PDGF-AA– and -BB–mediated chemotaxis, indicating that VEGFA_{165} competes with PDGF ligands for PDGFR occupancy. Because both MSCs and HDFs were shown to express abundant VEGF-A transcript, it is tempting to speculate that autocrine expression of VEGF-A may act to regulate PDGF-induced chemotaxis in these cell types.

The demonstration that, in the absence of VEGFRs, VEGF can use PDGFR-mediated signaling in both MSCs and HDFs, suggests the intriguing possibility that under certain circumstances, VEGF may have an impact on a wider range of target cells than previously recognized.

VEGF-A is a crucial factor in promoting the recruitment and proliferation of vascular cells during both physiological and pathological angiogenesis and neovascularization (Pierce et al., 1995; Carmeliet and Jain, 2000). The local oxygen concentration controls the expression of VEGF, which is mediated, at least in part, by the transcription factor, hypoxia-inducible factor 1 (Forsythe et al., 1996). Therefore, in pathological hypoxic microenvironments, such as tumorigenesis (Carmeliet and Jain, 2000), disease progression is often associated with increased VEGF-A and vascular remodeling. MSCs are actively recruited during tumor neovascularization (Annabi et al., 2003; Aghi and Chiocca, 2005) and engraft into established tumor lesions (Hung et al., 2005), forming the basis for novel therapeutic approaches. Thus, VEGF-A/PDGFR signaling, especially during tissue hypoxia, is likely to be an important determinant in the recruitment and proliferation of MSCs and other PDGFR-positive cells.

Materials and methods

Cell culture

Human MSCs from normal bone marrow of 20- and 26-yr-old females and 18-, 22-, and 24-yr-old males (Cambrex), HUVECs from 35- and 29-yr-old females, and a pooled batch of HUVECs and HDFs from 23- and 32-yr-old males (Cascade Biologics) were maintained as previously described (Ball et al., 2004). MSCs were analyzed at passage 4, whereas HUVECs and HDFs were analyzed at passage 6. All were grown in serum-free medium for 24 h before analysis. The MSCs used in this study express a wide range of smooth muscle cell markers, including the smooth muscle cell–selective marker smoothelin-B (Ball et al., 2004), and can also differentiate into osteoblast, chondrocyte, and adipocyte lineages (McBeath et al., 2004). They are positive for CD29, CD44, CD105, and CD166, but negative for hematopoietic cell markers CD14, CD34, and CD45. We have also demonstrated that they are negative for the specific pericyte marker 3G5 (Nayak et al., 1988; Ball et al., 2007).

Growth factors and inhibitors

All growth factors, PDGF-AA (221-AA), PDGF-BB (220-BB), TGF-β_1 (240-B), VEGF-A_{165} (293-VE), and VEGF-A_{121} (298-VS), were obtained from R&D Systems. Three different batches of VEGF-A_{165} were used during this study, all containing BSA carrier protein (50 μg BSA/1 μg cytokine). We excluded the possibility that the VEGF-A may contain contaminant PDGF-BB (which binds to both PDGFRs). Immunoblot analysis (using anti–PDGF-B) readily detected 1 ng PDGF-B, but 100 ng VEGF-A_{165} produced no PDGF-B immunoreactivity, indicating that any potential PDGF-BB contamination must be $<$1 ng (Fig. S2). However, the minimum concentration of PDGF-BB that induced a detectable PDGFRα or PDGFRβ tyrosine phosphorylation response was $\geq$5 ng and 2 ng, respectively (Fig. S2). Thus, any potential contamination of $<$1 ng PDGF-BB (in 100 ng VEGF-A_{165}) would not induce a detectable PDGFR tyrosine phosphorylation response.

In addition, VEGF-A_{165} from two different suppliers (Invitrogen and Autogen Bioclear) was also tested, and both showed similar biological effects to the VEGF-A_{165} obtained from R&D Systems.

Anti–human PDGFRα (MAB322) and PDGFRβ (AF385) antibodies were used to specifically neutralize PDGFRs, whereas anti–human VEGFR1 (AF321) and VEGFR2 (MAB3572) antibodies were used to specifically neutralize VEGFR1 and VEGFR2 (R&D Systems). PDGFR tyrosine kinase was inhibited using PDGFR tyrosine kinase inhibitor III (50 nM PDGFRα IC_{50}; PDGFRβ IC_{50}, 80 nM with $IC_{50} \geq 30$ μM for EGFR, FGFR, Src, PKA, and PKC; Matsuno et al., 2002; Calbiochem). VEGFR2 tyrosine kinase was inhibited using VEGFR2 inhibitor V ($IC_{50} < 2$ nM with $IC_{50} > 50$ μM for VEGFR1, EGFR, FGFR1 and PDGFRβ; Endo et al., 2003; Calbiochem).

Semiquantitative RT-PCR

Semiquantitative RT-PCR was performed as previously described (Ball et al., 2004). Each primer pair was designed using the same parameters, resulting in similar Tm values (58.8–60.0) and product lengths as shown. VEGFR-1 (99-bp), forward (5′-GCGACGTGTGGTCTTACG-3′) and reverse (5′-GGCGACTGCAAAAGTCCT-3′); VEGFR-2 (81-bp), forward (5′-CATCCAGTGGGCTGATGA-3′) and reverse (5′-TGCCACTTCCAAAAGCAA-3′); VEGFR-3 (87-bp), forward (5′-GATGCGGGACCGTATCTG-3′) and reverse (5′-ATCCTCGGAGCCTTCCAC-3′); VEGF-A (98-bp), forward (5′-CACCCATGGCAGAAGGAG-3′) and reverse (5′-CACCAGGGTCTCGATTGG-3′); NP-1 (77-bp), forward (5′-GCAGTGGCTCCTGGAAGA-3′) and reverse (5′-AGTCGCCTGCATCCTGTC-3′); NP-2 (83-bp), forward (5′-ATTCGGGATGGGGACAGT-3′) and reverse (5′-CCCGAGGAGATGATGGTG-3′); and GAPDH (71-bp), forward (5′-AAGGGCATCCTGGGCTAC-3′) and reverse (5′-GTGGAGGAGTGGGTGTCG-3′). An additional pair of primers for all three VEGFRs (VEGFR1-3) that was designed to different sequence regions were also used (primer sequences not shown).

Flow cytometry

For single-color flow cytometry, MSCs, HUVECs, or HDFs (4×10^6 cells/ml) were incubated with either PE-conjugated anti–human VEGFR1-PE (FAB321P), VEGFR2-PE (FAB357P), or VEGFR3-PE (FAB3492P) antibodies, or control anti–IgG_1-PE antibody (IC002P; R&D Systems). VEGFR1 (MAB4711), VEGFR2 (MAB3572), VEGFR3 (MAB3491) antibodies, or control anti-IgG_1 (MAB002) antibody (R&D Systems) were also used after secondary labeling with a FITC secondary antibody (Dako Cytomation). HDFs were also incubated with either anti–human PDGFRα-PE (sc-21789PE) or PDGFRβ-PE (sc-19995PE) antibodies (Santa Cruz Biotechnology). For each sample, 100,000 cells were counted using a FACscan cytometer (Becton Dickinson) at a flow rate of <200 events/s.

Migration assay

Cell migration was determined using a modified Boyden chamber assay. Cell culture filter inserts of 8 μm pore size, 6.5 mm diam (Becton Dickinson), were coated on the underside with 10 μg/ml fibronectin in PBS, overnight at 4°C. MSCs (1×10^5) were added to the upper chamber with 10 or 20 ng/ml growth factors in the lower chamber and cells allowed to migrate to the membrane underside for 5 h at 37°C in a humidified atmosphere of 5% CO_2 in air. In some experiments, cells were preincubated with receptor neutralization antibodies or kinase inhibitors (10 μg/ml anti-VEGFR1 or anti-VEGFR2 neutralization antibodies, 100 nM VEGFR2 tyrosine kinase inhibitor [VEGFR2-TK], 2 μM PDGFR tyrosine kinase inhibitor [PDGFR-TK], and 10 μg/ml anti-PDGFRα or -PDGFRβ neutralization antibodies) for 30 min at 37°C before growth factor exposure. After migration, cells on the upper membrane surface were removed and migratory cells on the membrane underside were fixed using 5% (wt/vol) glutaraldehyde and stained using 0.1% (wt/vol) crystal violet solution. Filter inserts were inverted and the number of migratory cells on the membrane underside (cells/field using a 10× NA 0.3 Olympus UPlanF1 objective lens) was determined, at room temperature, by visualizing the crystal violet–stained cells directly on insert undersides by phase-contrast microscopy, without use of fluorochromes (BX51; Olympus). Images were captured using a computerized imaging system (MetaMorph imaging v 5.0; Molecular Devices) and CoolSNAP (Photometrics) camera system.

Proliferation assay

MSCs (2,000 cells/well) in growth medium were seeded in 96-well plates and incubated with 10 ng/ml growth factors at 37°C in a humidified atmosphere of 5% CO_2 in air. Experiments were also conducted using MSCs pretreated with 10 μg/ml receptor neutralization antibodies for 30 min before growth factor addition. At the end of each time point, a CyQuant cell proliferation assay kit (Invitrogen) was used to detect MSC proliferation. Cells were treated in situ according to the manufacturer's protocol. To generate a standard curve, a serial dilution of MSCs (2,000–20,000) were also aliquoted into separate wells and treated the same as sample cells. Plates were read using a scanning multiwell fluorometer at a wavelength of 480 nm, and cell numbers were calculated using the standard curve for each plate.

RTK array analysis

A human Phospho-RTK Array kit (R&D Systems), which has a greater sensitivity than immunoprecipitation analysis, was used to simultaneously detect the relative tyrosine phosphorylation levels of 42 different RTKs in untreated or growth factor–treated MSC lysates. Each array contains duplicate validated control and capture antibodies for specific RTKs. MSCs cultured for 24 h in serum-free medium were stimulated with 20 ng/ml growth factors for 10 min at 37°C in a humidified atmosphere of 5% CO_2 in air, and then immediately placed on ice, washed twice with chilled PBS, and isolated using chilled lysis buffer (20 mM Tris-HCl, pH 8.0, 150 mM NaCl, 1% NP-40, 2.5 mM EDTA, 1 mM sodium orthovanadate, 10% glycerol, 10 μg/ml aprotinin, 10 μg/ml leupeptin, and 1 mM phenylmethylsulfonyl fluoride). Total protein concentration was quantitated using a BCA assay kit (Pierce Chemical Co.). RTK array analysis was performed according to the manufacturer's protocol. In brief, array membranes were blocked, incubated with 500 μg MSC lysate overnight at 4°C, washed, and incubated with anti–phosphotyrosine-HRP for 2 h at room temperature, washed again, and developed with ECL Western blotting detection reagent (GE Healthcare), and RTK spots were visualized using Kodak XAR film. Average pixel density of duplicate spots were determined by Gene Tools v3 software (Syngene), with values normalized against corner duplicate phosphotyrosine-positive control spots, which were assigned a value of 100.

siRNA transfection

MSCs (5×10^5 cells), together with 3-μg siRNAs, were transfected by electroporation using a human Nucleofector kit (Amaxa) and cultured overnight in growth medium. Validated siRNAs, which were functionally tested to provide ≥70% target gene knockdown, were used for PDGFRα and PDGFRβ knockdown and a scrambled siRNA control (QIAGEN).

Phosphorylated PDGFR immunoprecipitation and sandwich ELISAs

Cells were isolated using ice-cold lysis buffer and 100 μg lysates precleared using 10% (wt/vol) protein A–Sepharose (GE Healthcare), and then incubated with monoclonal anti–human PDGFRα (MAB1264) or PDGFRβ (MAB1263; R&D Systems) overnight at 4°C. Immune complexes were isolated by incubation with 10% (wt/vol) protein A–Sepharose for 2 h. Immunoblot analysis was performed as previously described (Ball et al., 2004), using a monoclonal anti–human antibody for phosphorylated tyrosine (PY99; sc-7020; Santa Cruz Biotechnology). Human phospho-PDGFRα, phospho-PDGFRβ and soluble PDGF-BB levels were all detected by ELISA kits, performed according to the manufacturer's protocol (R&D Systems).

Cross-linking analysis of growth factor association with PDGFRs

After stimulation of MSCs in serum-free conditions with growth factor, 1 mM 3, 3′-Dithiobis[sulfosuccinimidyl propionate] (DTSSP; Pierce Chemical Co.) was directly added to the medium and incubated for 30 min at room temperature, and the cross-linking reaction was quenched using 20 mM Tris, pH 7.5, for 15 min at room temperature. DTSSP is a membrane-impermeable thiol-cleavable reagent that is used for cross-linking molecules at the cell surface. PDGFRs were immunoprecipitated from cell lysates using anti–human PDGFRα (MAB1264) or PDGFRβ (MAB1263; R&D Systems). Proteins conjugated to PDGFR–DTSSP complexes were dissociated by adding 5% β-mercaptoethanol and boiling for 5 min. Growth factors associated with PDGFRs were resolved by SDS-PAGE and detected by immunoblot analysis, as previously described (Ball et al., 2004), using the following corresponding monoclonal anti–human antibodies: VEGF-A (MAB293), PDGF-B (MAB220), or TGF-β_1 (MAB240; R&D Systems).

Statistical analysis

In all quantitation experiments, results are expressed as the mean ± the SD. Statistical differences between sets of data were determined by using a paired *t* test on SigmaPlot 8.0 software, with $P < 0.05$ considered significant.

Online supplemental material

Fig. S1 shows that inhibition of PDGFRα or PDGFRβ attenuated VEGF-A–induced MSC proliferation. Fig. S2 shows that VEGF-A contained no detectable PDGF-BB contamination. Fig. S3 shows that VEGF-A did not change soluble PDGF-BB levels.

This work was funded by the UK Centre for Tissue Engineering (Medical Research Council, Biotechnology and Biological Sciences Research Council, and Engineering and Physical Sciences Research Council). C.M. Kielty is a Royal Society-Wolfson Research Merit Award holder.

Submitted: 16 August 2006
Accepted: 4 April 2007

References

Abedin, M., Y. Tintut, and L. Demer. 2004. Mesenchymal stem cells and the artery wall. *Circ. Res.* 95:671–676.

Aghi, M., and E.A. Chiocca. 2005. Contribution of bone marrow-derived cells to blood vessels in ischemic tissues and tumors. *Mol. Ther.* 12:994–1005.

Annabi, B., Y.-T. Lee, S. Turcotte, E. Naud, R.R. Desrosiers, M. Champagne, N. Eliopoulos, J. Galipeau, and R. Beliveau. 2003. Hypoxia promotes murine bone-marrow-derived stromal cell migration and tube formation. *Stem Cells.* 21:337–347.

Ball, S.G., A.C. Shuttleworth, and C.M. Kielty. 2004. Direct cell contact influences bone marrow mesenchymal stem cell fate. *Int. J. Biochem. Cell Biol.* 36:714–727.

Ball, S.G., A.C. Shuttleworth, and C.M. Kielty. 2007. Platelet-derived growth factor receptor-alpha is a key determinant of smooth muscle alpha-actin filaments in bone marrow-derived mesenchymal stem cells. *Int. J. Biochem. Cell Biol.* 39:379–391.

Benjamin, L.E., I. Hemo, and E. Keshet. 1998. A plasticity window for blood vessel remodeling is defined by pericyte coverage of the preformed

endothelial network and is regulated by PDGF-B and VEGF. *Development*. 125:1591–1598.

Betsholtz, C. 2004. Insight into the physiological functions of PDGF through genetic studies in mice. *Cytokine Growth Factor Rev.* 15:215–228.

Carmeliet, P., and R.K. Jain. 2000. Angiogenesis in cancer and other diseases. *Nature*. 407:249–257.

Cho, N.K., L. Keyes, E. Johnson, J. Heller, L. Ryner, F. Karim, and M.A. Krasnow. 2002. Developmental control of blood cell migration by the *Drosophila* VEGF pathway. *Cell*. 108:865–876.

Cross, M.J., J. Dixelius, T. Matsumoto, and L. Claesson-Welsh. 2003. VEGF-receptor signal transduction. *Trends Biochem. Sci.* 28:488–494.

Duchek, P., K. Somogyi, G. Jekely, S. Beccari, and P. Rorth. 2001. Guidance of cell migration by the Drosophila PDGF/VEGF receptor. *Cell*. 107:17–26.

Endo, A., S. Fukuhara, M. Masuda, T. Ohmori, and N. Mochizuki. 2003. Selective inhibition of vascular endothelial growth factor receptor-2 (VEGFR-2) identifies a central role for VEGFR-2 in human aortic endothelial cell responses to VEGF. *J. Recept. Signal Transduct. Res.* 23:239–254.

Fiedler, J., N. Etzel, and R.E. Brenner. 2004. To go or not to go: migration of human mesenchymal progenitor cells stimulated by isoforms of PDGF. *J. Cell. Biochem.* 93:990–998.

Forsythe, J.A., B.-H. Jiang, N.V. Iyer, F. Agani, S.W. Leung, R.D. Koos, and G.L. Semenza. 1996. Activation of vascular endothelial growth factor gene transcription by hypoxia-inducible factor 1. *Mol. Cell. Biol.* 16:4604–4613.

Fredriksson, L., H. Li, and U. Eriksson. 2004. The PDGF family: four gene products form five dimeric isoforms. *Cytokine Growth Factor Rev.* 15:197–204.

Furumatsu, T., Z.N. Shen, A. Kawai, K. Nishida, H. Manabe, T. Oohashi, H. Inoue, and Y. Ninomiya. 2003. Vascular endothelial growth factor principally acts as the main angiogenic factor in the early stage of human osteoblastogenesis. *J. Biochem. (Tokyo)*. 133:633–699.

Galmiche, M.C., V.E. Koteliansky, J. Briere, P. Herve, and P. Charbord. 1993. Stromal long-term marrow cultures are mesenchymal cells that differentiate following a vascular smooth muscle differentiation pathway. *Blood*. 82:66–76.

Gluzman-Poltorak, Z., T. Cohen, Y. Herzog, and G. Neufeld. 2000. Neuropilin-2 and neuropilin-1 are receptors for 165-amino acid long form of vascular endothelial growth factor (VEGF) and of placenta growth factor-2, but only neuropilin-2 functions as a receptor for the 145 amino acid form of VEGF. *J. Biol. Chem.* 275:18040–18045.

Heldin, C.H., and B. Westermark. 1999. Mechanism of action and in vivo role of platelet-derived growth factor. *Physiol. Rev.* 79:1283–1316.

Holmes, D.I., and I. Zachary. 2005. The vascular endothelial growth factor (VEGF) family: angiogenic factors in health and disease. *Genome Biol.* 6:209–219.

Hung, S.-C., W.-P. Deng, W.K. Yang, R.-S. Liu, C.-C. Lee, T.-C. Su, R.-J. Lin, D.-M. Yang, C.-W. Chang, W.-H. Chen, et al. 2005. Mesenchymal stem cell targeting of microscopic tumors and tumor stroma development monitored by noninvasive In vivo positron emission tomography imaging. *Clin. Cancer Res.* 11:7749–7756.

Kashiwakura, Y., Y. Katoh, K. Tamayose, H. Konishi, N. Takaya, S. Yuhara, M. Yamada, K. Sugimoto, and H. Daida. 2003. Isolation of bone marrow stromal cell-derived smooth muscle cells by a human SM22α promoter. *Circulation*. 107:2078–2081.

Kim, D.H., K.H. Yoo, K.S. Choi, J. Choi, S.-Y. Choi, S.-E. Yang, Y.-S. Yang, H.J. Im, K.H. Kim, H.L. Jung, et al. 2005. Gene expression profile of cytokine and growth factor during differentiation of bone marrow-derived mesenchymal stem cell. *Cytokine*. 31:119–126.

Kondo, K., S. Hiratuska, E. Subbalakshmi, H. Matsushime, and M. Shibuya. 1998. Genomic organization of the flt-1 gene encoding for vascular endothelial growth factor (VEGF) receptor-1 suggests an intimate evolutionary relationship between the 7-Ig and the 5-Ig tyrosine kinase receptors. *Gene*. 208:297–305.

Matsuno, K., M. Ichimura, T. Nakajima, K. Tahara, S. Fujiwara, H. Kase, J. Ushiki, N.A. Giese, A. Pandey, R.M. Scarborough, et al. 2002. Potent and selective inhibitors of platelet-derived growth factor receptor phosphorylation. 1. Synthesis, structure-activity relationship, and biological effects of a new class of quinazoline derivatives. *J. Med. Chem.* 45:3057–3066.

McBeath, R., D.M. Pirone, C.M. Nelson, K. Bhadrirju, and C.S. Chen. 2004. Cell shape, cytoskeletal tension, and RhoA regulate stem cell lineage commitment. *Dev. Cell*. 6:483–495.

Nayak, R.C., A.B. Berman, K.L. George, G.S. Eisenbarth, and G.L. King. 1988. A monoclonal antibody (3G5)-defined ganglioside antigen is expressed on the cell surface of microvascular pericytes. *J. Exp. Med.* 167:1003–1015.

Neufeld, G., T. Cohen, S. Gengrinovitch, and Z. Poltorak. 1999. Vascular endothelial growth factor (VEGF) and its receptors. *FASEB J.* 13:9–22.

Neufeld, G., T. Cohen, N. Shraga, T. Lange, O. Kessler, and Y. Herzog. 2002. The neuropilins: multifunctional semaphorin and VEGF receptors that modulate axon guidance and angiogenesis. *Trends Cardiovasc. Med.* 12:13–19.

Petrova, T.V., T. Makinen, and K. Alitalo. 1999. Signaling via vascular endothelial growth factor receptors. *Exp. Cell Res.* 253:117–130.

Pierce, E.A., R.L. Avery, E.D. Foley, L.P. Aiello, and L.E. Smith. 1995. Vascular endothelial growth factor/vascular permeability factor expression in a mouse model of retinal neo-vascularization. *Proc. Natl. Acad. Sci. USA*. 92:905–909.

Reigstad, L.J., J.E. Varhaug, and J.R. Lillehaug. 2005. Structural and functional specificities of PDGF-C and PDGF-D, the novel members of the platelet-derived growth factor family. *FEBS J.* 272:5723–5741.

Shimizu, K., S. Sugiyama, M. Aikawa, Y. Fukumoto, E. Rabkin, P. Libby, and R.N. Mitchell. 2001. Host bone-marrow cells are a source of donor intimal smooth muscle-like cells in murine aortic transplant arteriopathy. *Nat. Med.* 7:738–741.

Tarsitano, M., S. De Falco, V. Colonna, J.D. McGhee, and M.G. Persico. 2006. The *C. elegans* pvf-1 gene encodes a PDGF/VEGF-like factor able to bind mammalian VEGF receptors and to induce angiogenesis. *FASEB J.* 20:227–233.

Vitt, U.A., S.Y. Hsu, and A.J. Hsueh. 2001. Evolution and classification of cystine knot-containing hormones and related extracellular signaling molecules. *Mol. Endocrinol.* 15:681–694.

Wijelath, E.S., S. Rahman, M. Namekata, J. Murray, T. Nishimura, Z. Mostafavi-Pour, Y. Patel, Y. Suda, M.J. Humphries, and M. Sobel. 2006. Heparin-II domain of fibronectin is a vascular endothelial growth factor-binding domain: enhancement of VEGF biological activity by a singular growth factor/matrix protein synergism. *Circ. Res.* 99:853–860.

Yamazaki, Y., and T. Morita. 2006. Molecular and functional diversity of vascular endothelial growth factors. *Mol. Divers.* 10:515–527.

Yancopoulos, G.D., S. Davis, N.W. Gale, J.S. Rudge, S.J. Wiegand, and J. Holash. 2000. Vascular specific growth factors and blood vessel formation. *Nature*. 407:242–248.

Zachary, I., and G. Gliki. 2001. Signaling transduction mechanisms mediating biological actions of the vascular endothelial growth factor family. *Cardiovasc. Res.* 49:568–581.